ISSN 1810-2328, Journal of Engineering Thermophysics, 2024, Vol. 33, No. 2, pp. 384–396. © Pleiades Publishing, Ltd., 2024.

Identifying Transport Properties of Gas from Measurements of Heat Flux at Stagnation Point of Blunt Body. Technique and Experimental Results

A. V. Nenarokomov[1*], D. L. Reviznikov[2], S. A. Budnik[1], D. M. Titov[1], A. V. Morzhukhina[1], A. V. Netelev[1], and I. A. Borisenko[1]

[1] *Department of Space Systems and Rocket Engineering, Moscow Aviation Institute (National Research University), Moscow, Russia*

[2] *Department of Computational Mathematics and Programming, Moscow Aviation Institute (National Research University), Moscow, Russia*

Received December 11, 2023; in final form, May 17, 2024; accepted May 20, 2024

Abstract—In their previous work [1], the authors presented a method of identifying the characteristics of a gaseous medium from measurements of the heat flux absorbed by the surface of a blunt body in a gas flow. The identification problem was stated in an extreme formulation: the sought-for transport properties of a gaseous medium were determined via minimization of the objective function of the estimated and measured heat fluxes absorbed by the surface of a solid body. For minimization of the objective function, the Nelder–Mead method was used in combination with random restarts; the results of testing the algorithm in a model experiment are given. This paper presents the technique of conduction of experiment to verify the method for identification of the gas flow parameters. Experimental results are given for two different gas flow sources.

DOI: 10.1134/S1810232824020139

INTRODUCTION

Modern methods for designing systems for thermal control of space technology objects require the intensive use of mathematical and physical modeling methods. For instance, one of the most important stages in analysis of the characteristics of promising space reentry vehicles, as well as in creation of their digital models, is the joint solution of the problems of an external flow around an object and internal heat transfer [2, 3]. Very often, it is impossible to separate these two problems because the outer surface temperature has a significant influence on the heat transfer in the boundary layer. To adequately simulate the external flow around the object, it is necessary to know the characteristics of the oncoming gas flow. Direct measurement of the gas flow characteristics may be impossible for reasons related to the high temperatures in the boundary layer and destruction and melting of the material on the outer surface of the reentry vehicle. Nevertheless, some characteristics of the oncoming gas flow can assessed from indirect measurements (absorbed heat fluxes and surface temperatures of the body in the flow).

In [1], a method was proposed for calculation of the effective coefficients of viscosity and thermal conductivity of the oncoming flow gas. In this work, for verification of this method, a technique was developed for conducting an experiment on a gas-dynamic stand with application of sensors of absorbed heat fluxes on the basis of solving the inverse boundary-layer problem of heat transfer [4].

Identification of gas flow parameters can be reduced to solving the inverse heat transfer problem in the extremal formulation. In [1], for this purpose, minimization of the discrepancy between the calculated and measured values of the absorbed heat flux was used. The residual functional to minimize has the form

[*] Corresponding author. E-mail: aleksey.nenarokomov@mai.ru

$$J = \int_0^{\tau_{\max}} \int_0^L (q_w(x,t) - q_m(x,t))^2 dx dt, \tag{1}$$

where $\tau_{\max}$ is the time of observation, L is the characteristic size of the region of the forward stagnation point, $q_w(x,t) = (\lambda \frac{\partial T}{\partial y})_w$ is the estimated heat flux density, and $q_m(x)$ are the measured values of the heat flux to the surface.

The solution to his problem can be found by the Nelder–Mead method in combination with random restarts [5].

As already noted, measuring the heat flux density for calculation of functional (1) is an inverse boundary-layer problem of heat transfer. In [1], this problem was solved by the iterative regularization method [5] through the minimization of the objective functional of the discrepancy between measured and calculated temperatures at the points where the heat flow sensor thermocouples were installed:

$$J\left(q_m\left(\tau\right)\right) = \sum_{m=1}^{M} \int_0^{\tau_{\max}} \left(T[x_m,\tau) - f_m\left(\tau\right)\right)^2 d\tau, \tag{2}$$

where x_m is the coordinate of the mth thermocouple, $m = \overline{1,M}$, M being the number of thermocouples in the sensor; $T[x_m,\tau)$ is the calculated temperature value at the point x_m; $f_m\left(\tau\right)$ is the experimental temperature value at the same point.

Iterative minimization of functional (2) is performed by first-order gradient methods. The regularizing condition for stopping the iteration cycle is the last iteration number s^* chosen in accordance with the generalized residual principle [6]: $s^* : J\left(q_1^{s^*}\right) \cong \delta^2$, where δ^2 is the integral error of temperature measurement: $\delta^2 = \sum\limits_{m=1}^{M} \int\limits_{\tau_{\min}}^{\tau_{\max}} \sigma_m\left(\tau\right) d\tau$, and $\sigma_m\left(\tau\right)$ is the measurement dispersion.

Both in laboratory thermal studies and in acquisition of information on thermal loading during a flight experiment, a heat flow sensor made of the same material as the thermal protection coating (TPC) can be used [7]. For instant, measuring the heat flux on the surface of a body in a flow implies using sensors integrated into the TPC (see Figs. 1 and 2). In conduction of a flight experiment, subject to the operating conditions, the sensors may have thermocouples installed on the surface. Measuring the temperature on the surface makes it possible to increase the accuracy of the heat flux determination [8]. However, for example, at surface entrainment or melting of material, it is impossible to implement such measurement scheme [9].

Fig. 1. Heat flow sensor integrated into flexible TPC for inflatable space structures.

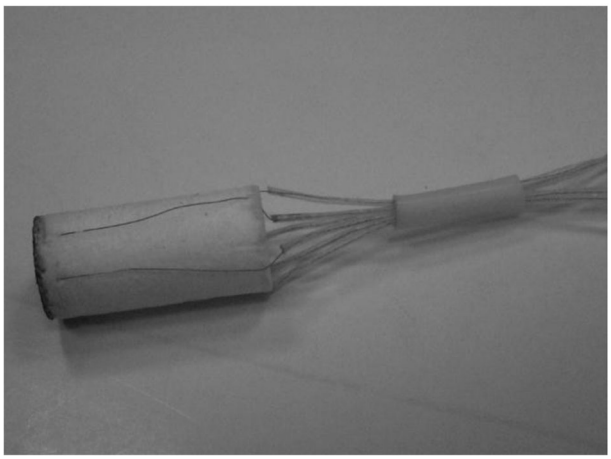

Fig. 2. Heat flow sensor integrated into quartz-fiber TPC.

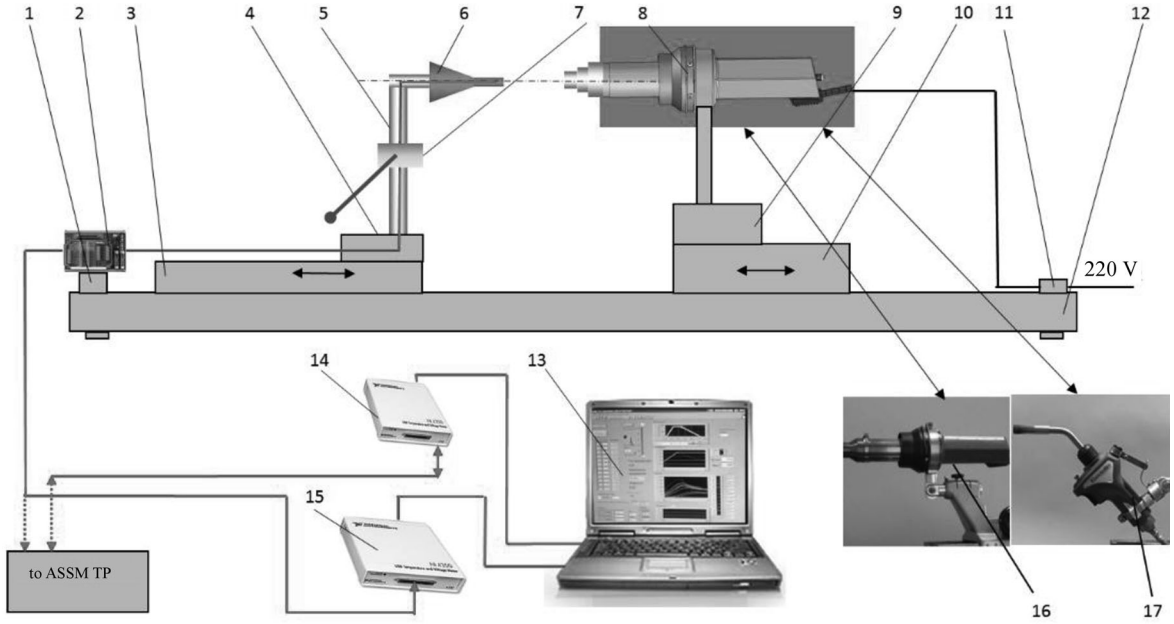

Fig. 3. Schematic diagram of setup UKN-1: 1—power connector, 2—connector box, 3—carriage for research object, 4—holder base, 5—holder for research object, 6—research object, 7—rotary unit for side feed of sensor, 8—replaceable heater, 9—heater base, 10—carriage for heater, 11—heater power connector, 12—setup base, 13—AS controller (NB), 14—AS measurement-and-control unit, 15—AS measurement unit, 16—replaceable electric air heater, 17—gas burner on MAPP gas.

EQUIPMENT AND TECHNIQUE OF EXPERIMENT

The experimental study under consideration to verify the technique for determination of the gas flow parameters [1] involved a small-sized convective heating setup UKN-1, developed at the Moscow Aviation Institute. The setup UKN-1 is intended for conduction of laboratory thermal tests for approbation and experimental refinement of technical and methodological means for diagnostics of thermal regimes of elements of heat-loaded structures in a real gas-dynamic experiments. Figure 3 presents the setup diagram, and Fig. 4 shows the appearance of the setup UKN-1, consisting of the following main components: base 12 with the fire pan; unit 4–5 for placement of the research object; unit 7 for side feed of sample; unit 8–9 for placement of replaceable heaters; autonomous automated system (AS) 13–15 of the setup.

The setup design enables adjustable coaxial (along the axis of the research object and the heater) placement of the main components with subsequent fixation of them. The unit for placement of

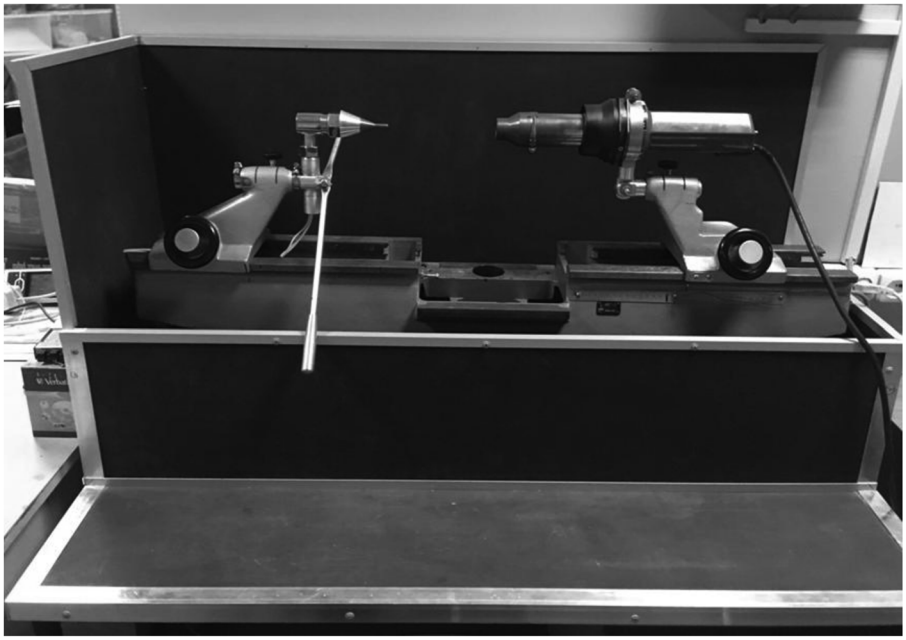

Fig. 4. Setup UKN-1 (with electric air heater).

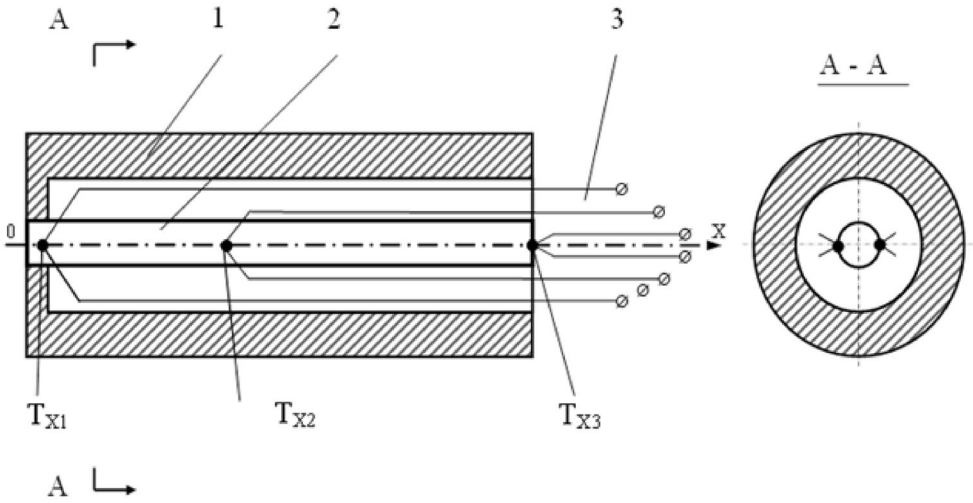

Fig. 5. Schematic diagram of one-dimensional heat flux density sensor with rod SE: 1—sensor body, 2—sensitive element, 3—thermocouple leads, TX1, TX2, TX3—thermocouples.

the research object can be moved coaxially relative to the setup base with subsequent fixation. Holder 5 provides coaxial placement and universal fastening of various types of research objects 6 (heat flow sensors, samples of structural elements, etc.), as well as the output of thermocouple wires from the sample and their protection from the influence of the high-temperature gas flow. The possible maximum dimensions of the research object with the thermocouple connector (length $\times$ height $\times$ width) are $5 \times 2 \times 2$ mm to $60 \times 50 \times 50$ mm. The unit for placement of replaceable heaters provides "manual" coaxial translation of the unit relative to setup base 12 and fixation of the unit in a selected position, as well as coaxial placement, positioning, and fastening of heaters. The heater is a high-performance industrial electric heater STEINEL HG5000E with replaceable nozzles and a high-temperature gas burner Castolin CT-27 on MAPP gas.

In this experimental study, the diagnostics of gas flows on the setup UKN-1 was done with non-stationary rod heat flow sensors. Figure 5 presents a schematic diagram of a one-dimensional heat

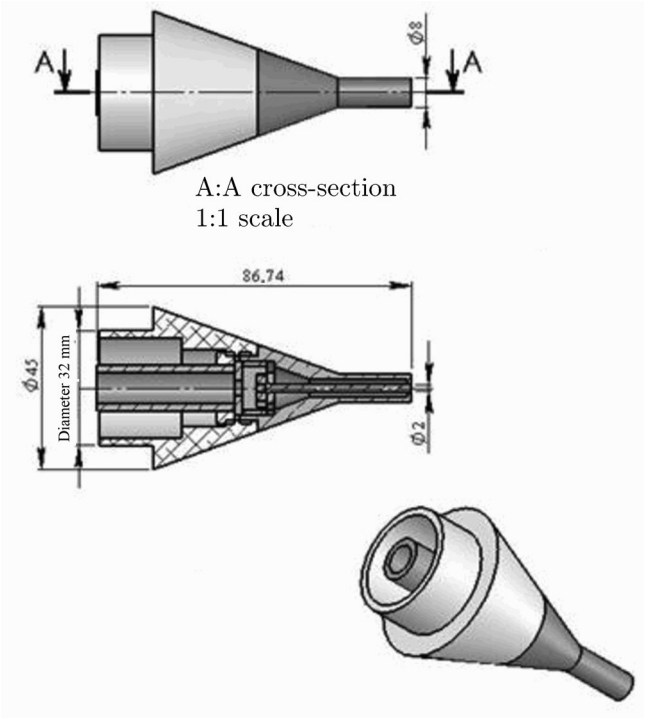

Fig. 6. General view of DTP-GD sensor.

Fig. 7. Heat flux density sensor DTP-GD-2.1.

flux density sensor with a rod sensitive element (SE). With readings of thermocouples T_{X1} and T_{X2} and T_{X3} temperature as the boundary condition, during the testing, the sensor implements a one-dimensional heating model. Figure 6 shows a general view of the one-dimensional non-stationary rod heat flow sensor DTP-GD, developed for this research program. The sensor consists of a cylindrical body with a conical "skirt"; cylindrical SE, which is inserted into the body with an air gap relative to the inner side surface of the body and is centered with tight fit into the hole in the end surface of the body. The length of the sensor SE is 40 mm; its diameter is 2 mm. The outer diameter of the cylindrical part of the body is 8 mm; the inner diameter is 6 mm. The protective casing is for smooth change in the direction of the hot gas flow, protection of the thermocouple thermoelectrodes and the sensor holder from the effects of the gas flow, as well as for fixation of the sensor in the holder. The sensing element and the sensor body are made of copper. The protective housing is made of aluminum alloy.

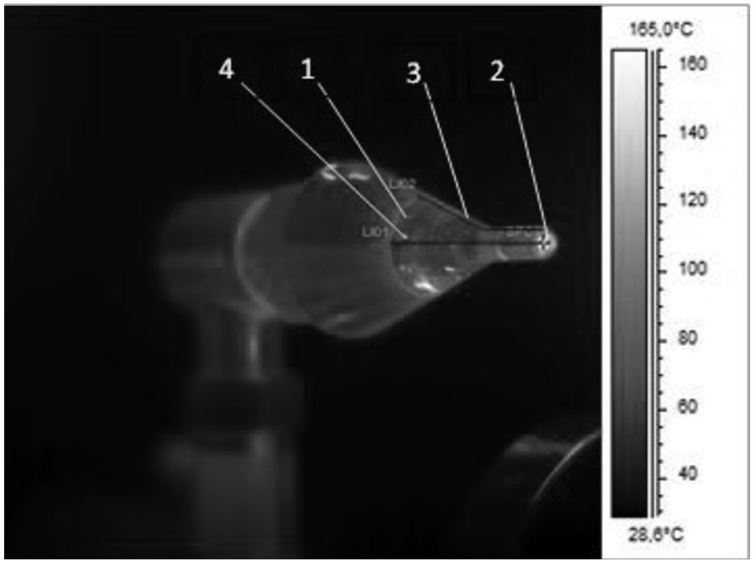

Fig. 8. Scheme of IR temperature measurements with virtual measuring instruments on IR image of sensor: 1—sensor, 2—measurement point SP01 on heated surface of SE, 3—measurement line LI02 on spill line, 4—measurement line LI01 on spill line.

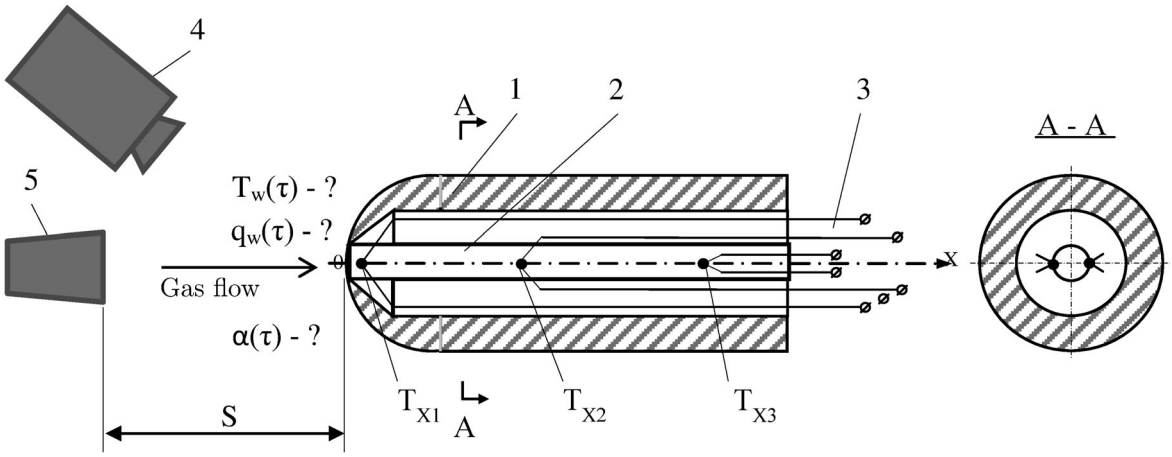

Fig. 9. Scheme of thermal tests on setup UKN-1 with heat flux sensor DTP-GD-2: 1—sensor body, 2—sensitive element (SE), 3—thermocouple leads, 4—thermal imaging camera, 5—heater nozzle, T_{X1}, T_{X2}, T_{X3}—thermocouples.

Table 1. Scheme of temperature measurements in sensors

Sensor	Measurement point/thermocouple	x_1 (mm)/(TX1)	x_2 (mm)/(TX2)	x_3 (mm)/(TX3)
DTP-GD-2.1	x_m/TXm	0.2/(TX1)	15.0/(TX2)	35.0/(TX3)
DTP-GD-2.2	x_m/TXm	0.25/(TX1)	15.8/(TX2)	33.5/(TX3)

Two sensors were manufactured by the scheme: DTP-GD-2.1 and DTP-GD-2.2. Figure 7 shows a photograph of one of the sensors.

Table 1 presents the scheme of temperature measurement (number and coordinates of measurement points) in the sensors. The coordinates of the measurement points x_m, $m = 1, \ldots, M$, are counted from the heated surface of sensor.

In SE cross sections with the coordinates x_1 and x_2, two thermocouples per cross section were

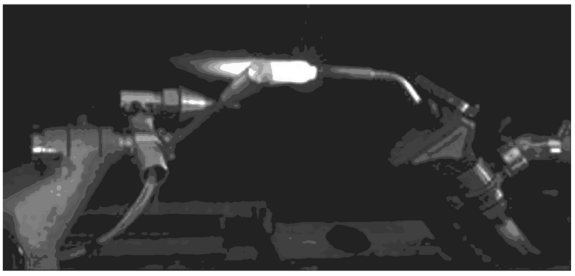

Burner has reached operating regime

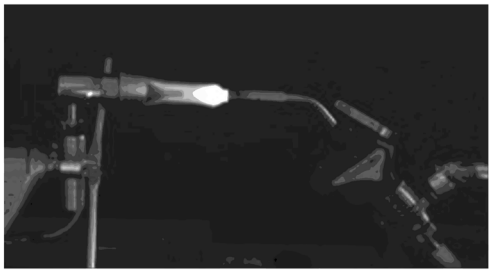

Sensor has been introduced into gas flow

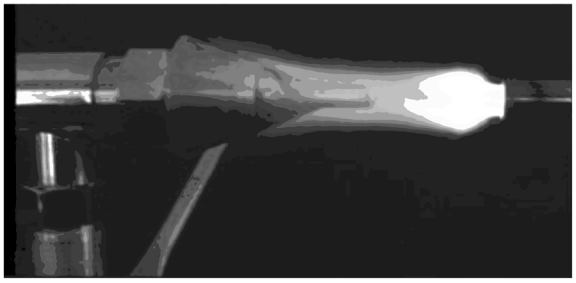

Sensor in gas flow at T_{1max}

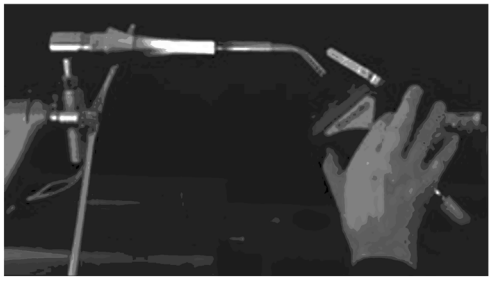

Burner turn-off

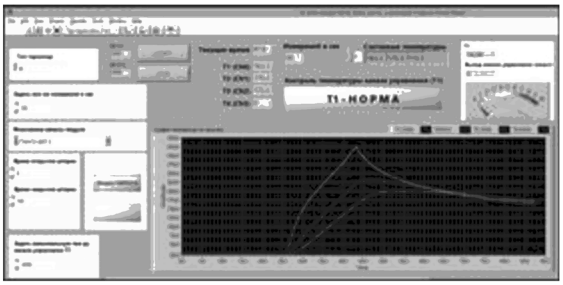

Main virtual panel of AS of setup

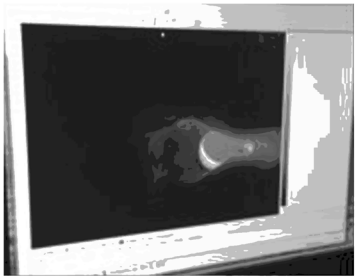

IR image of sensor on monitor of external controller of system FLIR

Fig. 10. Photographs of some characteristic moments of tests.

installed with an angular pitch of 180°. The readings of the two thermocouples in each cross section were averaged, and the resulting temperature values were used as the measurement result in the corresponding cross section. One thermocouple was installed in the cross section with the coordinate x_3. In this scheme, in the determination of the heat flux from the solution of the inverse boundary-layer problem of heat transfer, the temperature $f_3(\tau)$ is used as the boundary condition.

The equation of heat balance on the heated surface of the sensitive element (SE) of the sensor can be written in the following form:

$$q_w(\tau) = q_\lambda(\tau) + q_R(\tau), \tag{3}$$

where $q_w(\tau)$ is the convective heat flux, $q_\lambda(\tau)$ is the density of the conductive heat flux entering the SE (determined from the solution of the inverse boundary-layer problem of heat transfer), and $q_R(\tau)$ is the density of the thermal radiation flux from the heated surface of the SE.

The density of the flux emitted by the surface is determined from the relation

$$q_R(\tau) = \varepsilon\sigma T_W^4(\tau), \tag{4}$$

where $\varepsilon(T_W)$ is the blackness of the heated surface of the SE (in general, it depends on the temperature of the heated surface) and σ is the Stefan–Boltzmann constant.

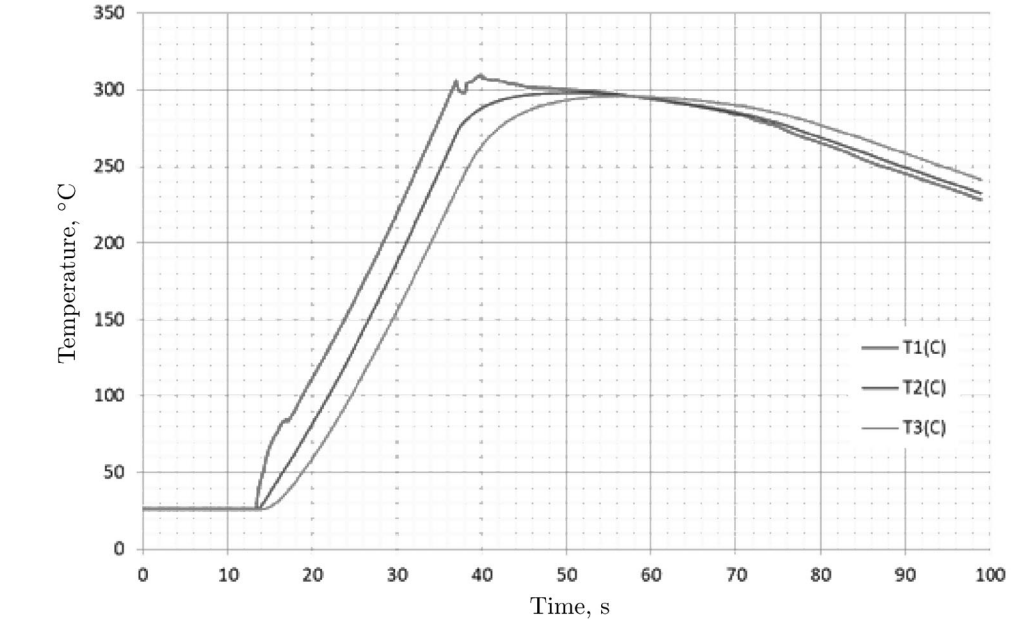

(a)

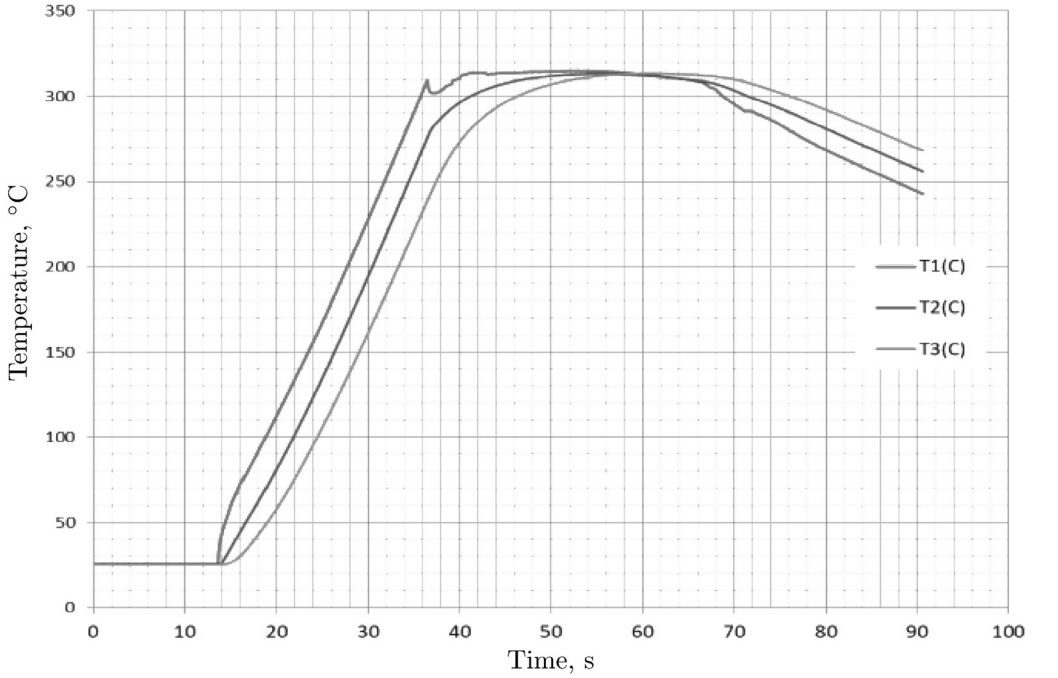

(b)

Fig. 11. Results of temperature measurements on UKN-1 with Castolin CT-27 burner on MAPP gas: (a) S = 50, (b) S = 30, (c) S = 70.

The temperature $T_W(\tau)$ can be determined via solving the inverse boundary-layer problem basing on the results of temperature measurements in the sensor SE. For assessment of the SE surface blackness $\varepsilon(T_W)$, the infrared thermal imaging system FLIR SC660 was used (Fig. 8) with application of the ThermaCAM^{TM} Researcher Professional 2.10 software [10].

Two series of experiments were carried out: with the electric heater and with the gas burner. In both series, the following main (target) measurements were performed:

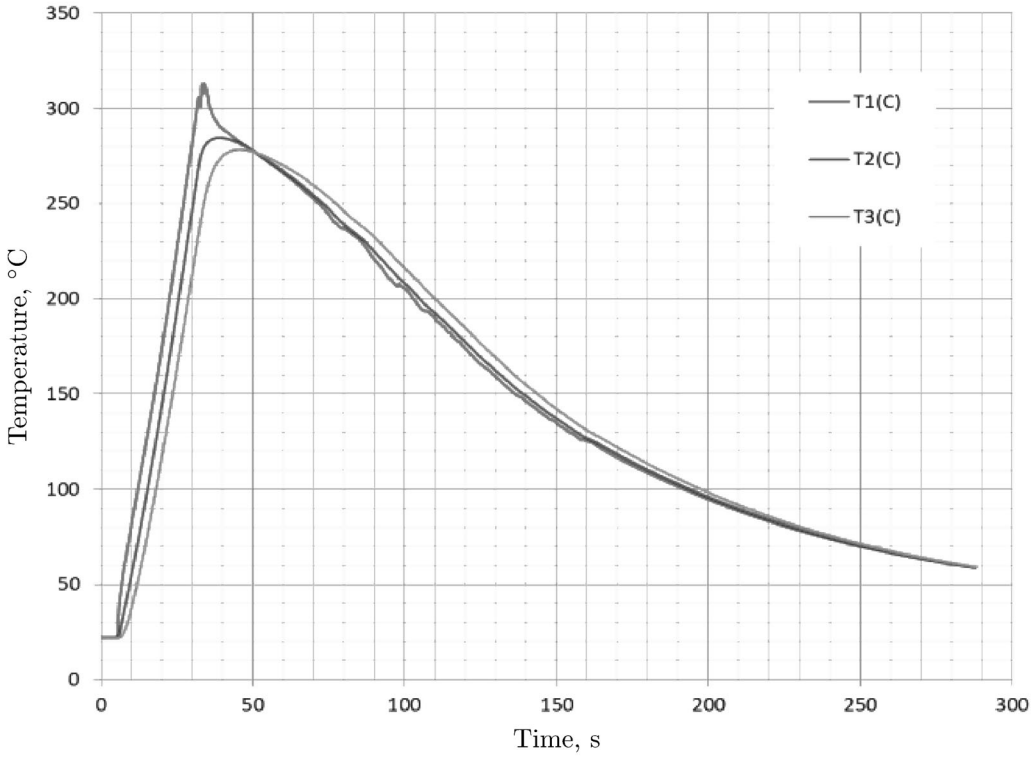

(c)

Fig. 11. (Contd.)

Table 2. Main test parameters of sensor DTP-GD-2.1 on setup UKN-1 with gas burner

No.	S, mm	τ_{s1}, s	τ_{e1}, s	$\Delta\tau$, s	T_{1max}, °C	$\Delta T_{12\,max}$, °C	$\Delta T_{23\,max}$, °C
1	70.0	5.56	34.08	28.52	313.08	34.0	34.0
2	50.0	13.44	39.83	26.39	309.39	33.0	36.0
3	30.0	13.63	34.47	22.84	310	34.0	36.0

Table 3. Main test parameters for sensor DTP-GD-2.2 on setup UKN-1 with air heater STEINEL HG5000E

No.	S, mm	τ_{s1}, s	τ_{e1}, s	$\Delta\tau$, s	T_{1max}, °C	$\Delta T_{12\,max}$, °C	$\Delta T_{23\,max}$, °C
1	50.0	3.76	686.4	682.0	290.41	22.68	14.78
2	30.0	16.69	244.93	228.24	300.54	30.28	18.60
3	50	11.49	129.08	117.59	302.19	35.18	22.28

—$f_m(\tau)$, $0 \le \tau \le \tau_{max}$, temperature variation over time at given points x_m, $m = 1, \ldots, M$, of the scheme of temperature measurements in the sensor SE (τ_{max} is the time of completion of the measurements).

—$T_W(\tau)$, $0 \le \tau \le \tau_{max}$, temperature variation on the heated surface of SE, measured with the infrared thermal imaging system.

The time of exposure of sensor to the heated gas flow was determined as $\Delta\tau = \tau s1 - \tau e1$, where $\tau s1$ is the time of insertion of the sensor into the gas flow, and $\tau e1$ is the time of the gas burner turn-off. The time $\tau s1$ was set subject to the time required for the heater to reach the operating

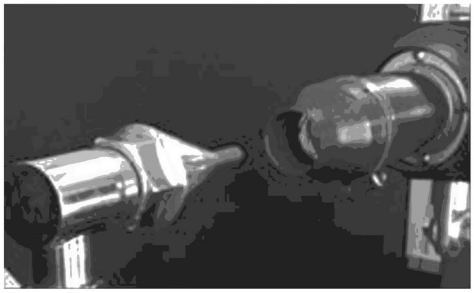

Sensor in gas flow at T_{1max}

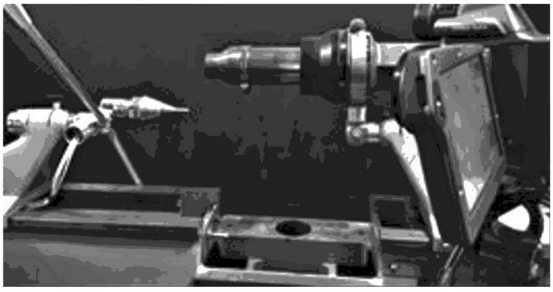

Sensor has been removed from gas flow. Free cooling of sensor

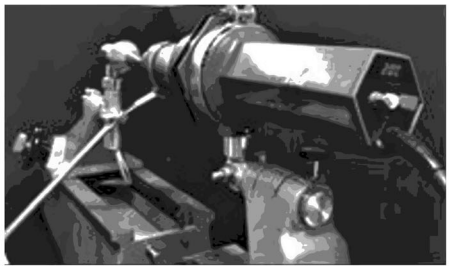

Forced cooling of sensor

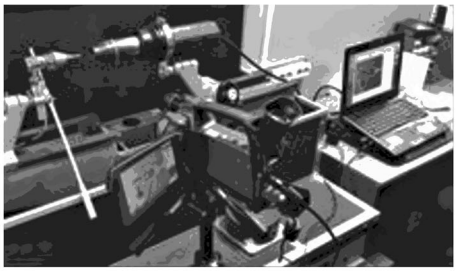

IR imaging with side-mounted thermal imaging camera

General view of setup UKN-1V during tests

Fig. 12. Photographs of some characteristic test moments.

regime and was up to 15 s. The time $\tau e1$ of the gas source switch-off was found from the time when the temperature of the heated surface of the sensor element reached the set value.

EXPERIMENTAL STUDIES ON SETUP UKN-1 WITH GAS BURNER

In the tests with the Castolin CT-27 burner on MAPP gas used as the gas source, three experiments were carried out with different distances S from the burner nozzle exit to the sensor DTP-GD-2.1. Table 2 presents the basic time and temperature data for the experiments with the gas burner.

Here T_{1max} is the maximum temperature, $\Delta T_{12\,max}$ and $\Delta T_{23\,max}$ are the maximum values of temperature differences at the test measurement points x_1, x_2 and x_2, x_3, respectively. Figure 10 shows photographs illustrating some characteristic moments of the tests.

Figure 11 shows thermograms obtained in the experiments. The coefficient $\varepsilon = 0.47$ on the heated surface of the sensor SE was calculated with the use of the ThermaCAM^{TM} Researcher software [10].

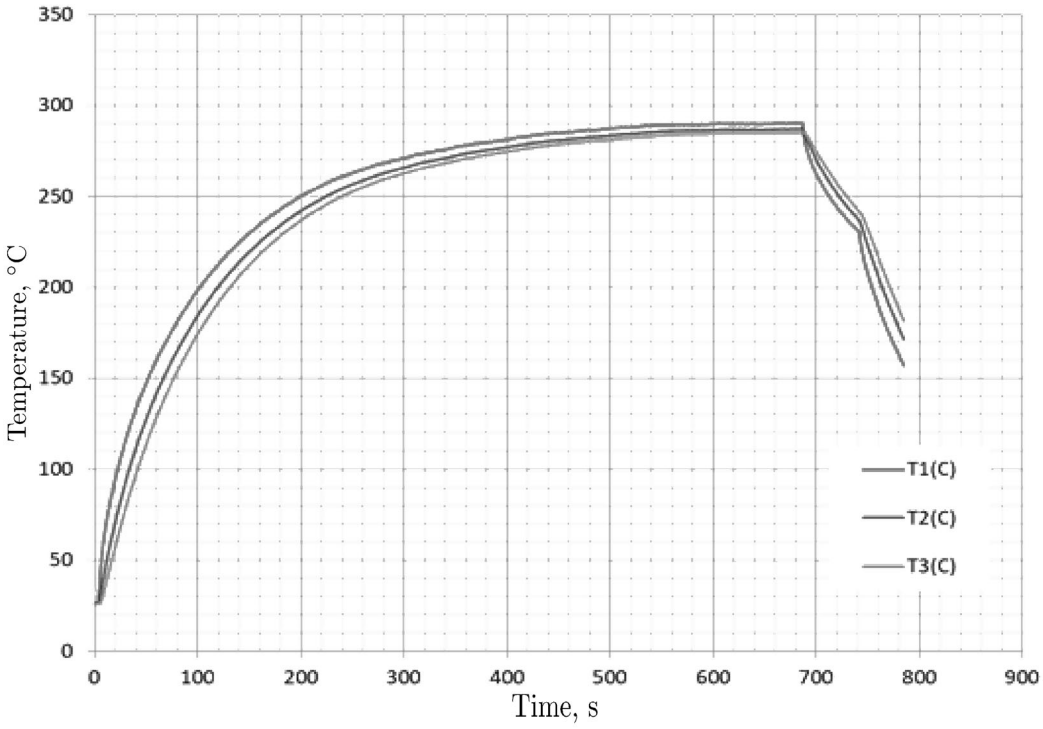

(a)

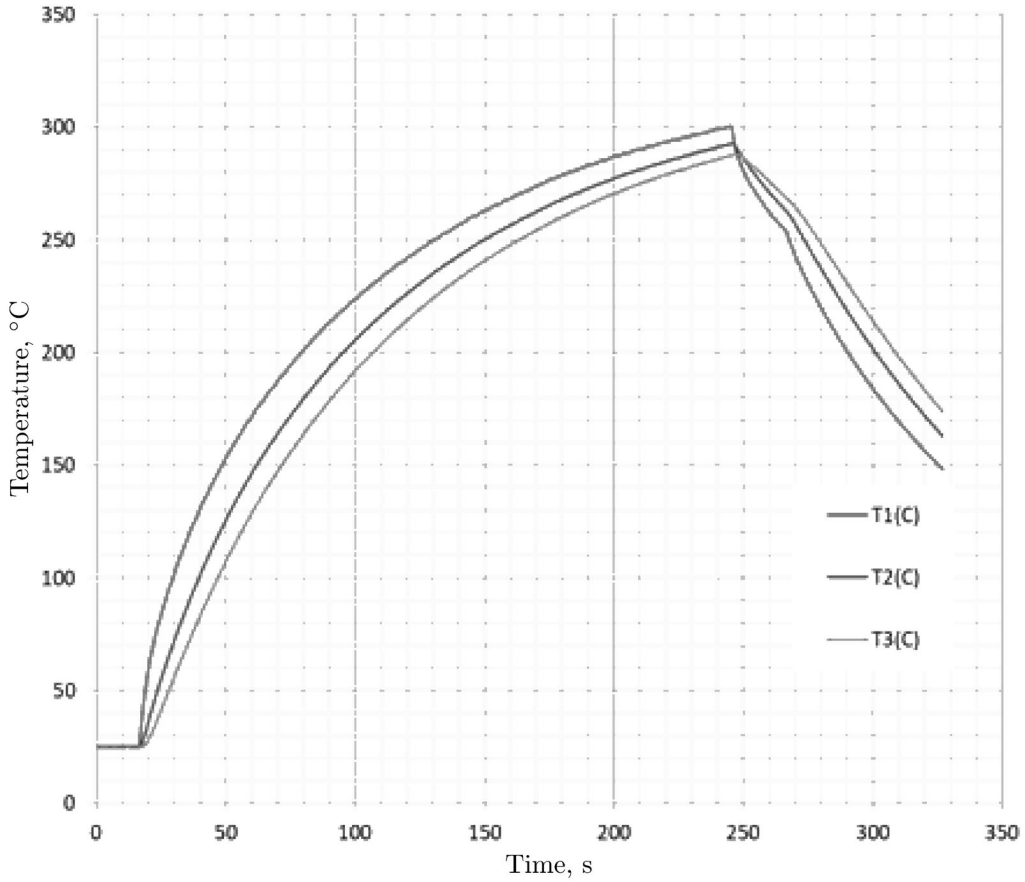

(b)

Fig. 13. Results of temperature measurements on UKN-1 with air heater STEINEL HG5000E: (a) S = 50, (b) S = 30, (c) S = 5.

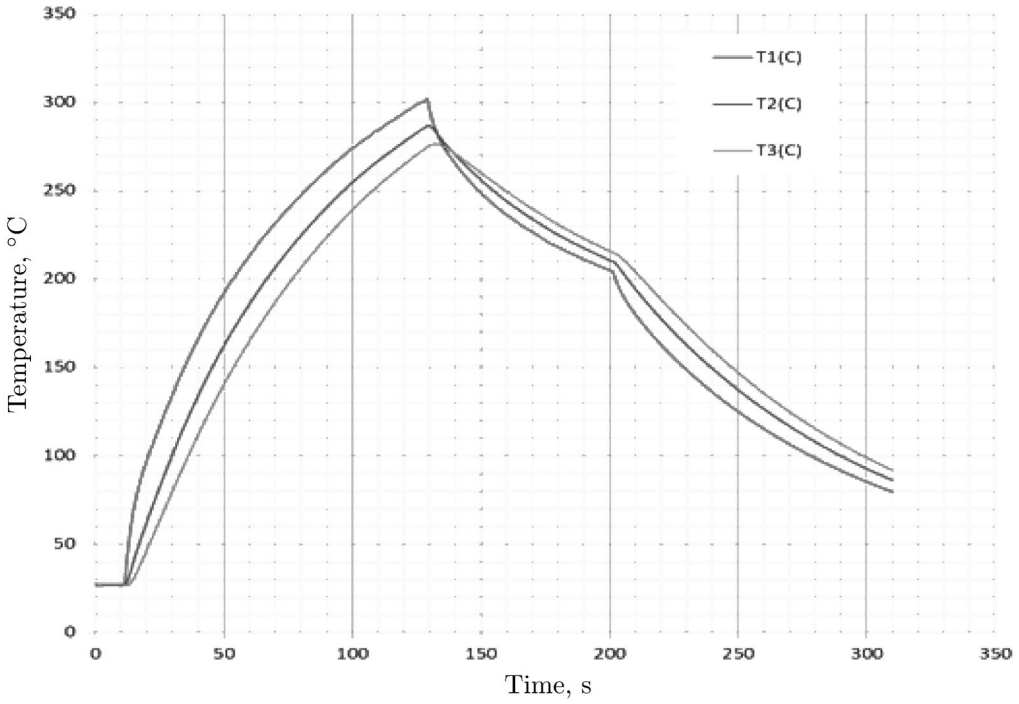

(c)

Fig. 13. (Contd.)

EXPERIMENTAL STUDIES ON SETUP UKN-1 WITH ELECTRIC AIR HEATER

The second stage involved the electric air heater STEINEL HG5000E with Ø50 mm nozzle. The stage included three experiments for different distances between the heater nozzle and the sensor DTP-GD-2.2. The tests were carried out at the constant air-flow temperature T = 600°C at the flow speed V = 0.2 m/s. Table 3 presents the main time and temperature data from the experiments with the electric air heater.

Figure 12 shows photographs illustrating some characteristic moments of the tests.

The calculated coefficient $\varepsilon = 0.431$ on the heated surface of the sensor SE. Figure 13 presents thermograms of the experiments.

CONCLUSIONS

The research carried out leads to the following main conclusions:

—in the analysis of the methods and means for determination of the thermal regime of heat-loaded structures, the main attention was paid to heat flux density sensors that implement the inverse boundary-layer problem of heat transfer to measure high-intensity thermal loads, including sensors integrated into the thermal protection of experimental spacecraft;

—the modernized setup UKN-1 with replaceable sources of convective heating and autonomous automated system for control, measurement, and collection and processing of experimental data with the novel non-stationary heat flow sensors DTP-GD with rod SEs was successfully used for thermal tests in various heating modes, which confirmed the performance and efficiency of the sensors;

—based on the results of the series of thermal tests, the initial data necessary for solving the problems of gas flow diagnostics using methods of the inverse boundary-layer problem of heat transfer were generated.

ACKNOWLEDGMENTS

The authors express their gratitude to A.G. Mednov, A.N. Ivanov, V.V. Samarin, and V.N. Yarotskii for their participation in the preparation and conduction of the experimental studies.

FUNDING

This work was supported by the Russian Science Foundation (project no. 21-19-00683).

CONFLICT OF INTEREST

The authors of this work declare that they have no conflicts of interest.

REFERENCES

1. Reviznikov, D.L., Neverova, D.A., Nenarokomov, A.V., Morzhukhina, A.V., and Chumakov, V.A., Identification of Gas Properties via Measurements of Absorbed Heat Flux, *J. Eng. Therm.*, 2022, vol. 31, pp. 248–260; https://doi.org/10.1134/S1810232822020060
2. Jung, J., Yee, K., and Jeong, S., Efficient Method for Heat Flux Calculations within Multidisciplinary Analyses of Hypersonic Vehicles, *Aerospace*, 2023, vol. 10, p. 846; https://doi.org/10.3390/aerospace10100846
3. Sun, J., Zhu, H., Xu, D., and Cai, G., Aerodynamic Thermal Simulation and Heat Flux Distribution Study of Mechanical Expansion Reentry Vehicle, *Aerospace*, 2023, vol. 10, p. 310; https://doi.org/10.3390/aerospace10030310
4. Alifanov, O.M., Artyukhin, E.A., and Nerokomov, A.V., *Obratnye zadachi v issledovanii slozhnogo teploobmena* (Inverse Problems in the Study of Complex Heat Transfer), Moscow: Yanus-K, 2009.
5. Nelder, J.A. and Mead, R., A Simplex Method for Function Minimization, *Comput. J.*, 1965, vol. 7, pp. 308–313.
6. Alifanov, O.M., Artyukhin, E.A., and Rumyantsev, S.V., *Ekstremal'nye methody resheniya nekorrektnykh zadach i ikh primenenie k obratnym zadacham teploobmena* (Extremal Methods of Solving Incorrect Problems and Their Application to the Inverse Problems of heat Transfer), Moscow: Nauka, 1988.
7. Alifanov, O.M., Budnik, S.A., Morzhukhina, A.V., Nenarokomov, A.V., Netelev A.V., and Titov, D.M., Heat-Flux Sensors Integrated into the Structure of Thermal Protection Coatings, *J. Engin. Phys. Thermophys.*, 2018, vol. 91, no. 1, pp. 26–39.
8. Budnik, S.A. and Nerokomov, A.V., Optimal Measurement Planning in Determination of Characteristics of Heat Loading of Bodies with Moving Boundaries, *TVT*, 1997, vol. 35, no. 3, pp. 453–457.
9. Saavedra, J. and Cuadrado D.G., Thermal Sensor Allocation for Effective and Efficient Heat Transfer Measurements in Transportation Systems, *Sensors*, 2023, vol. 23, p. 2803; https://doi.org/10.3390/s23052803
10. *Programma ThermaCAM*^{TM} *Researcher. Rukovodstvo pol'zovatelya* (Program ThermaCAM^{TM} Researcher. User Manual), Moscow: OAO PERGAM INZHINIRING, 2005.